User's Manual for Finite Element Pavement Response Analysis Software TTI-PAVE

ICAR-508

Oct. 30th, 2009

Background

A finite element program was developed to calculate the responses of the pavement under traffic load. The finite element procedure and the code was originally derived by Owen and Hinton (1980) using elasto-plastic formulation. This software is developed to analyze an axisymmetric problem with material nonlinearity. Liu modified the program by developing a mesh generation algorithm, implementation of several constitutive models and non-symmetric solutions. Later in 2000 Park made another set of modification to the software to incorporate stress dependent Poisson ratio nonlinear analysis using load increments. Adu-Osie later modified the program to incorporate cross-anisotropy in the formulations. Adu-Osie implemented Uzan's model presented in equation 1 instead of the nonlinear elasto-plastic model for pavement analysis.

$$E_y = k_1 Pa\left(\frac{I_1}{Pa}\right)^{k_2}\left(\frac{\tau_{oct}}{Pa}\right)^{k_3} \quad (1)$$

Where

E_y= resilient modulus in y directions,

G_{xy}= shear modulus in xy plane;

I_1=First invariant of the stress tensor;

τ_{oct}=shear stress on octahedral plane;

Pa=atmospheric pressure; and

k-parameters= fitting parameters determined from stress path tests.

The formulation of equation (1) is general. It can easily be downgraded to a linear elastic model when the model parameters k_2 and k_3 are set to zero. Apart from nonlinear model parameters (k_2 and k_3), modular ratios (E_x/E_y) and G_{xy}/E_y) and the ratio of the horizontal to vertical Poisson ratio (ν_{xx}/ν_{xy}) are needed for anisotropic analysis.

It should be noted here that the convergence of the iterative algorithm is very sensitive to the value of the Poisson ratios. Proper selection of this ratio deems necessary to guarantee convergence.

The finite element program adopts a compression-is-negative sign convention. Gravity stresses due to the weight of the overburden materials and residual stresses were not included in this finite element analysis. Figure 1 shows schematic representation of the boundary conditions of the finite element software.

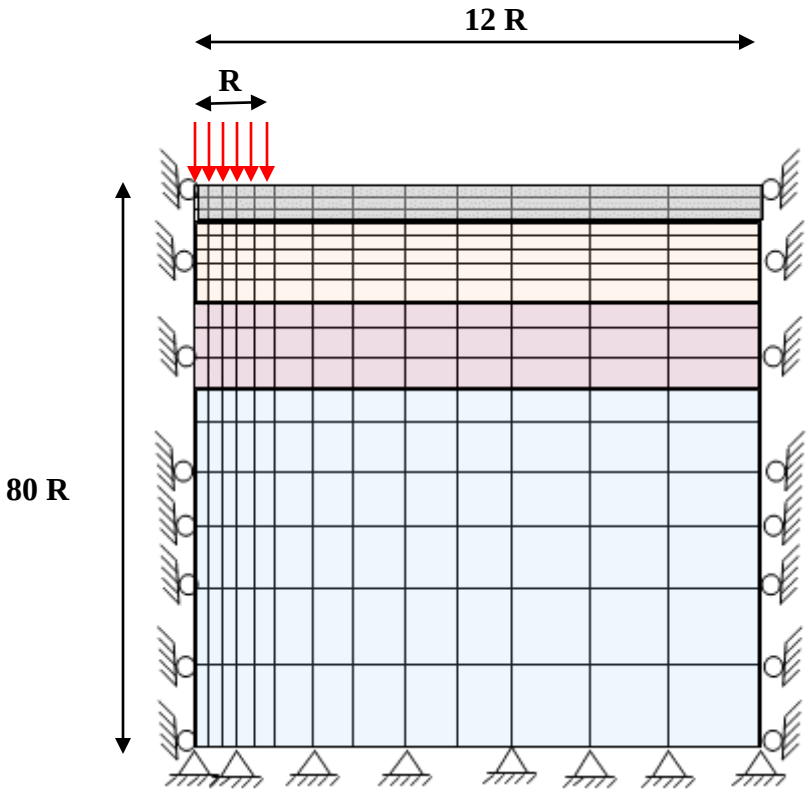

Figure 1 Schematic Representation of Boundary Conditions

General Properties Module

In the *General Properties* module user can select the number of layers (three or four layers), tire configuration (single or dual) and loading information. By clicking on the apply bottom the data entered in this module will be saved in the system and the user can proceed to the next module namely *Layer Properties*.

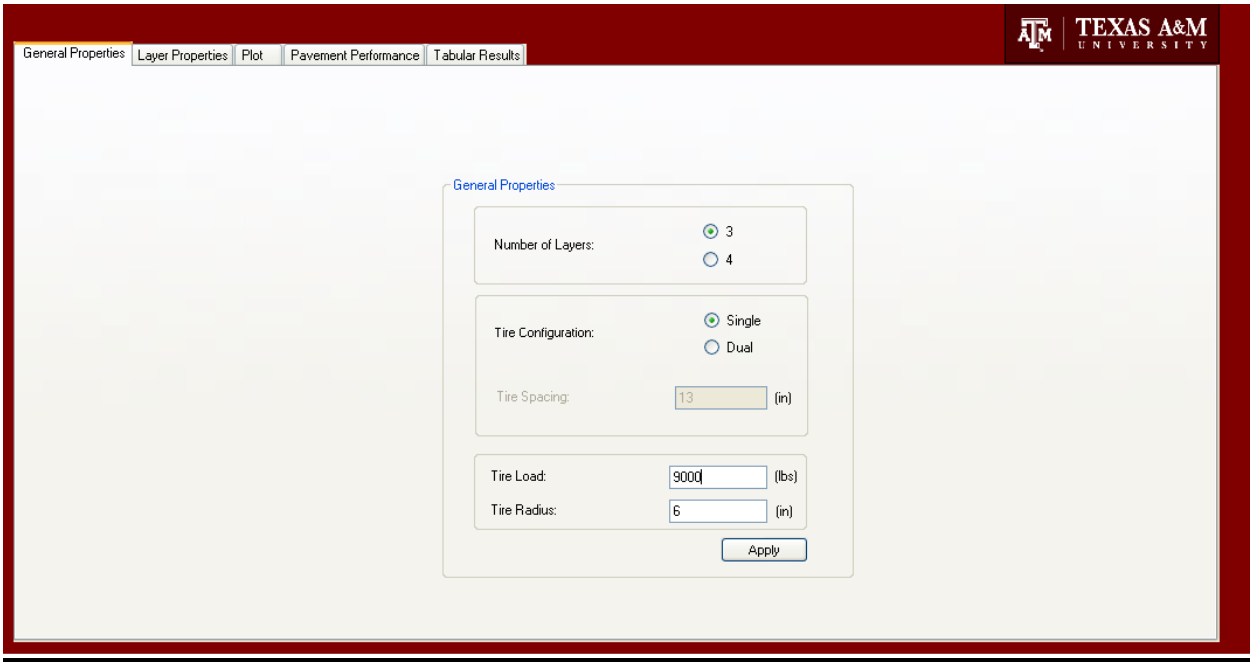

Figure 2 General Properties Module

Layer Properties Module

In this module user can define the material type (linear isotropic, nonlinear isotropic, linear anisotropic and nonlinear anisotropic) and the material properties. Level of anisotropy is characterized by three ratios: E_x/E_y, G_{xy}/E_y and ν_{xx}/ν_{xy} , if this ratio is one the material is called isotropic otherwise it is anisotropic. Nonlinearity of the system is characterized by the k_2 and k_3 parameters. k_2 is the exponent of the hardening parameter that models the stiffening effect of the geomaterials under load. k_3 captures the softening behavior in the model that simulates the loss of load bearing capacity of the system due to high shear forces and damage to the material.

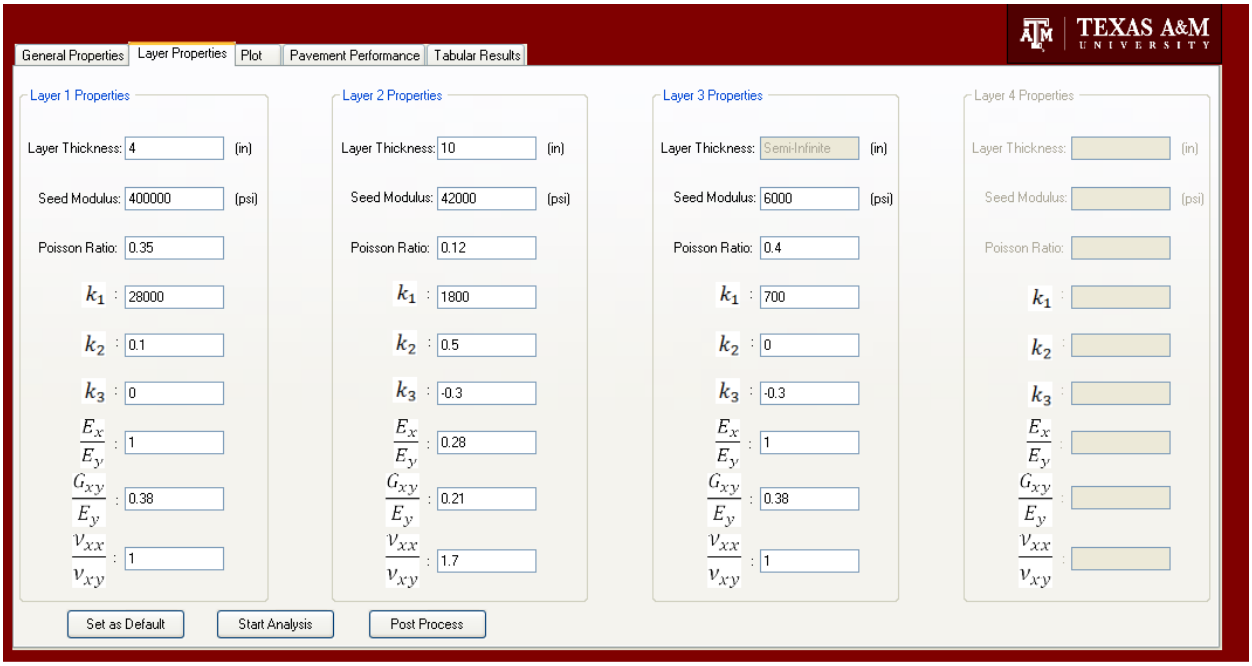

Figure 3 Layer Properties Module

Click on the *Start Analysis* button when the data entry for all the required fields was done. At this point the program iteratively calculates the mechanical responses of the pavement layers. When program reaches convergence the *Post Process* bottom will be activated as shown in figure 4.

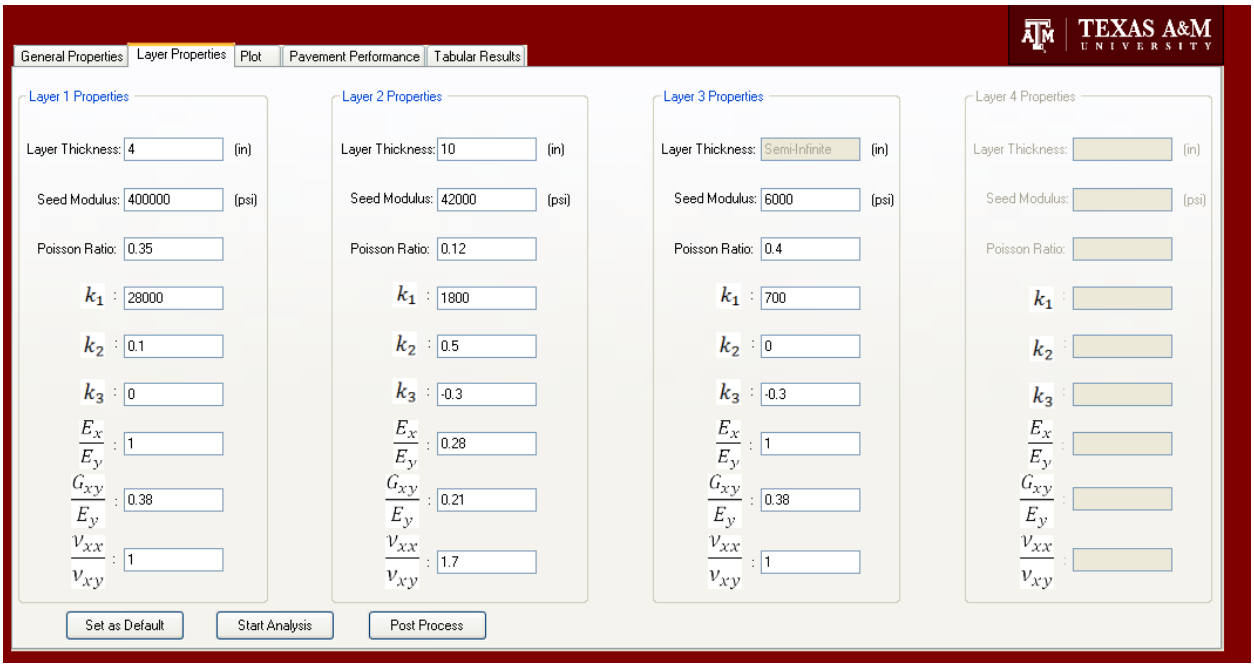

Figure 4 Post Process Activation

Plot Module

User can select the type of mechanical response from the drop down menue at the right side of the screen. The range of the axes (radial distance from the load on the horizontal axes and pavement depth on the vertical axes) can be manulay selected to costomize the plots.

The effect of radial distances on the distribution of the stresses and strains can be demonstrated by plotting responses at different radial offesets on the same graph. Figure 7 shows the reduction of vertical stresses induced on the pavement layers with radial offset from the centerline of the load. User can narrow down the range for R_{min} and R_{max} to view the results at specific radial offset.

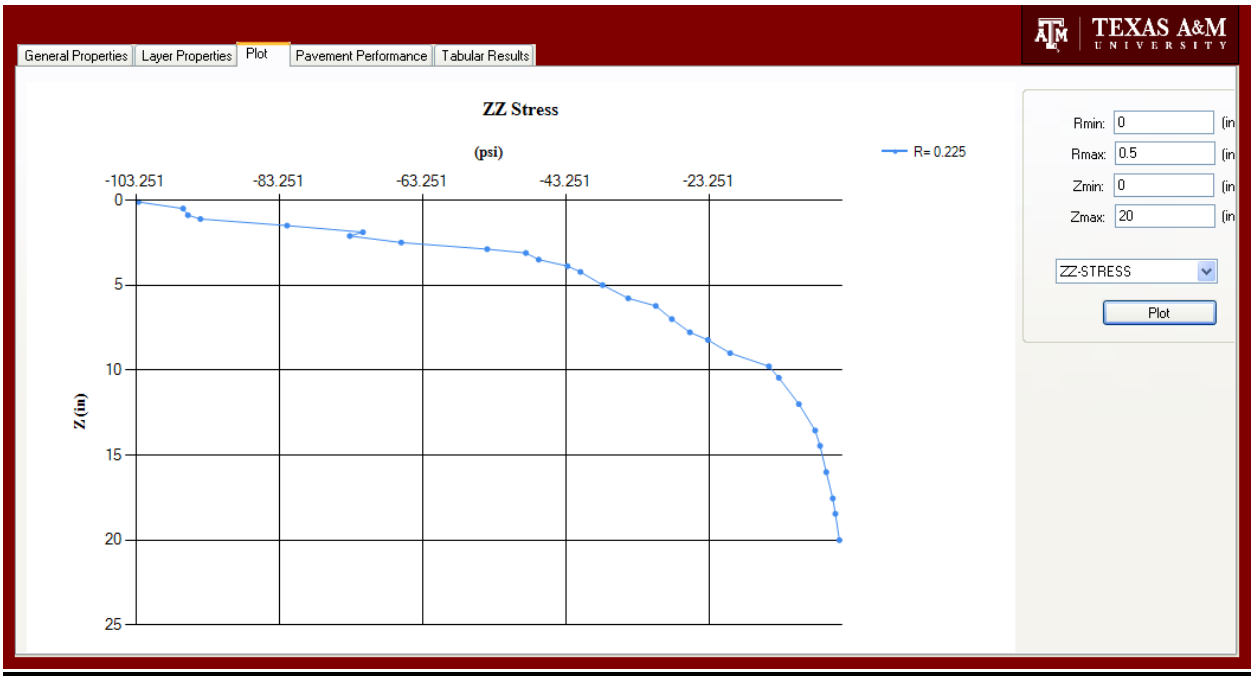

Figure 5 Sample Output; Distribution of Vertical Stresses in the Pavement Layers

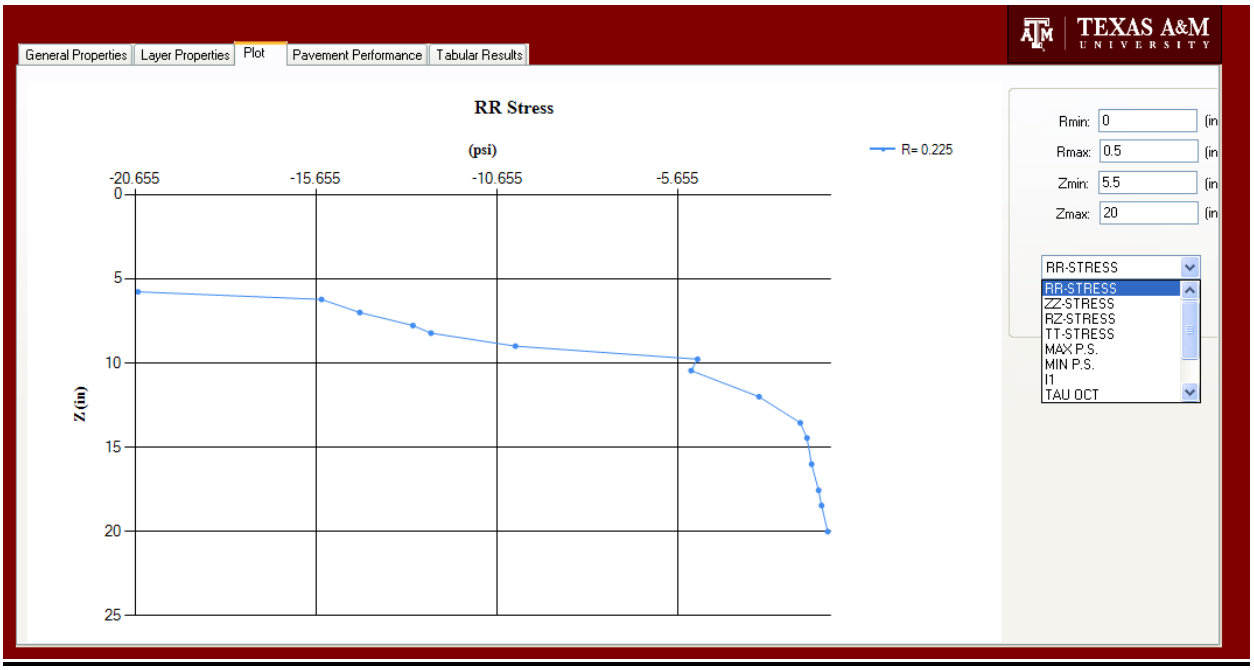

Figure 6 Sample Output; Distribution of Radial Stresses in the Base and Subgrade

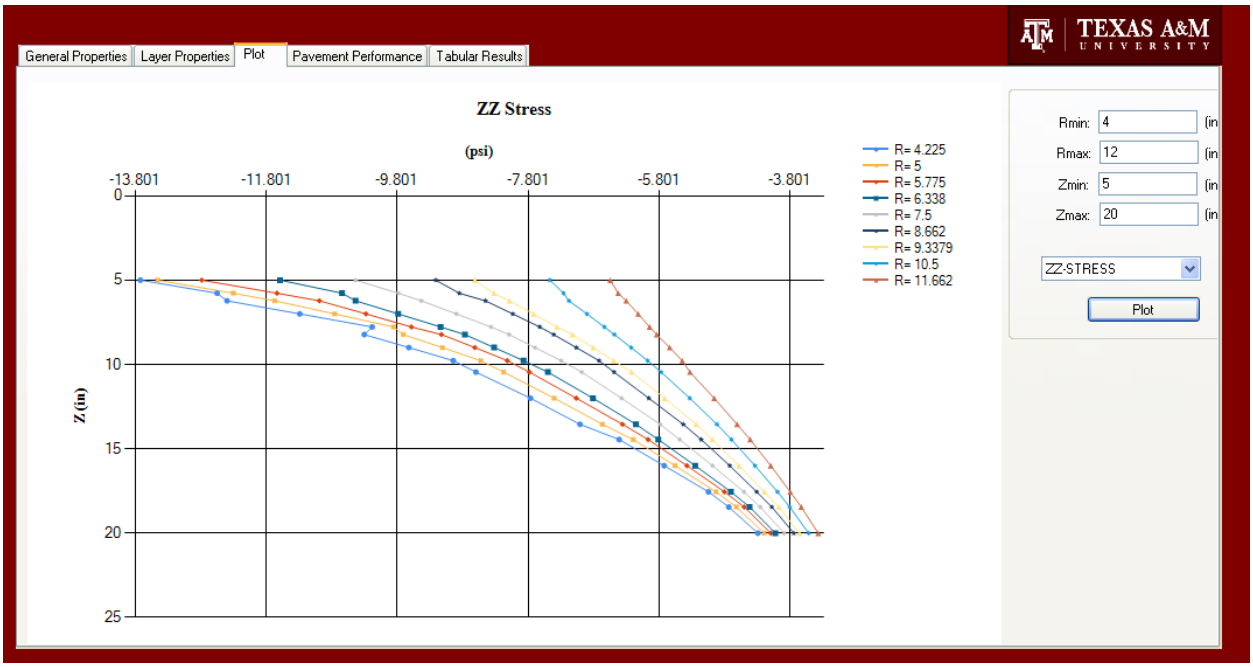

Figure 7 Sample Output; Countor Plot for Vertical Stresses

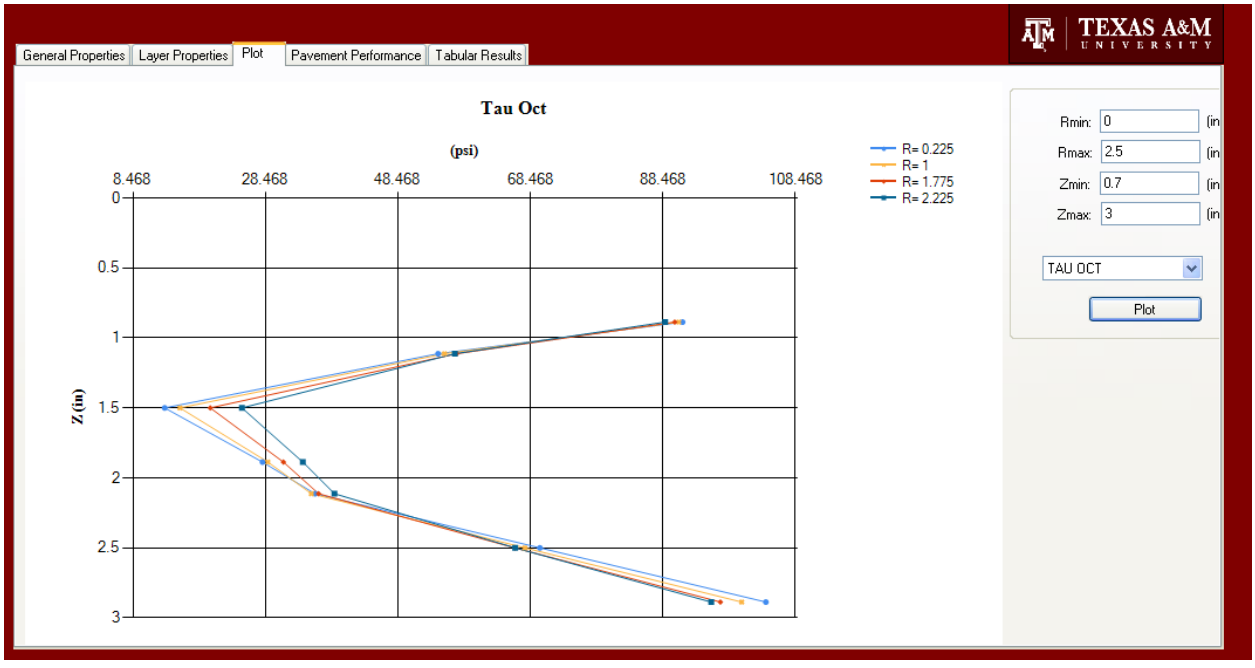

Figure 8 Sample Output; Countor Plot for Octahedral Shear Stresses in the Aspphalt Layer

Tabular Results Module

User can view the results in tabular format by selecting the *tabular results* tab. This allows for more flexibility in post processing of the pavement responses. Tabular results can be easily exported into Microsoft Excel™ for further analysis. Figure 9 shows a sample of output data in tabular format.

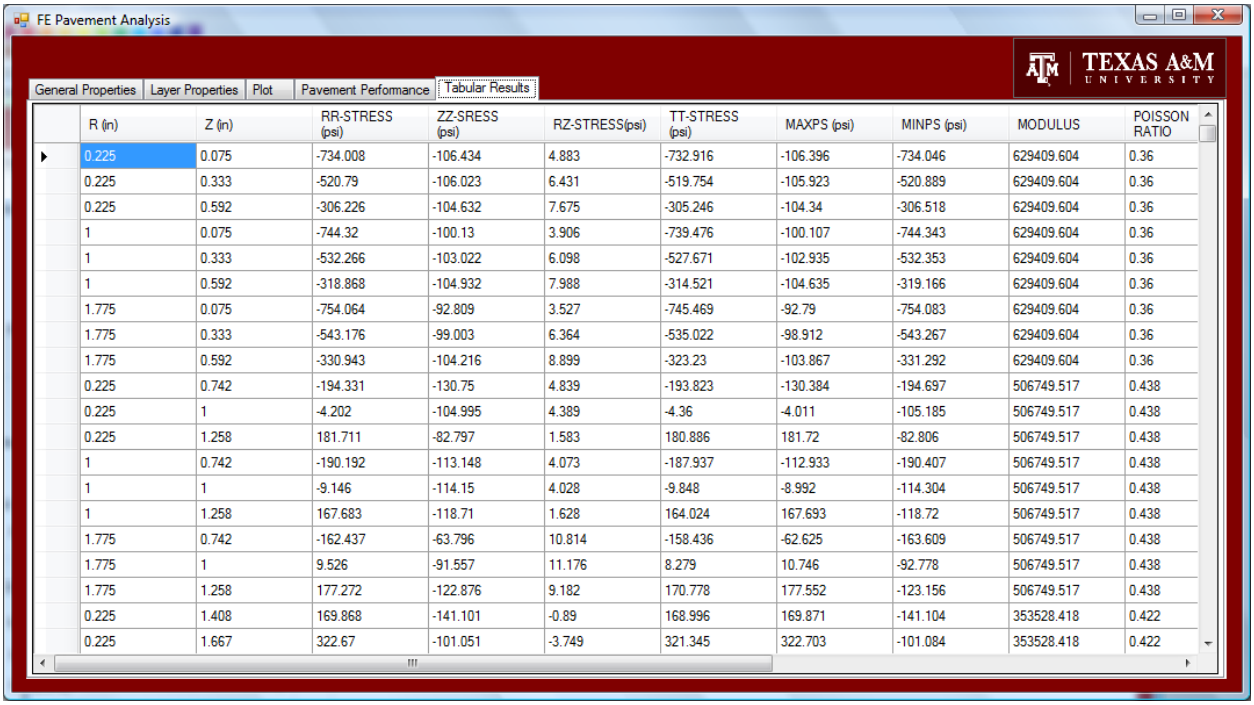

R (in)	Z (in)	RR-STRESS (psi)	ZZ-SRESS (psi)	RZ-STRESS(psi)	TT-STRESS (psi)	MAXPS (psi)	MINPS (psi)	MODULUS	POISSON RATIO
0.225	0.075	-734.008	-106.434	4.883	-732.916	-106.396	-734.046	629409.604	0.36
0.225	0.333	-520.79	-106.023	6.431	-519.754	-105.923	-520.889	629409.604	0.36
0.225	0.592	-306.226	-104.632	7.675	-305.246	-104.34	-306.518	629409.604	0.36
1	0.075	-744.32	-100.13	3.906	-739.476	-100.107	-744.343	629409.604	0.36
1	0.333	-532.266	-103.022	6.098	-527.671	-102.935	-532.353	629409.604	0.36
1	0.592	-318.868	-104.932	7.988	-314.521	-104.635	-319.166	629409.604	0.36
1.775	0.075	-754.064	-92.809	3.527	-745.469	-92.79	-754.083	629409.604	0.36
1.775	0.333	-543.176	-99.003	6.364	-535.022	-98.912	-543.267	629409.604	0.36
1.775	0.592	-330.943	-104.216	8.899	-323.23	-103.867	-331.292	629409.604	0.36
0.225	0.742	-194.331	-130.75	4.839	-193.823	-130.384	-194.697	506749.517	0.438
0.225	1	-4.202	-104.995	4.389	-4.36	-4.011	-105.185	506749.517	0.438
0.225	1.258	181.711	-82.797	1.583	180.886	181.72	-82.806	506749.517	0.438
1	0.742	-190.192	-113.148	4.073	-187.937	-112.933	-190.407	506749.517	0.438
1	1	-9.146	-114.15	4.028	-9.848	-8.992	-114.304	506749.517	0.438
1	1.258	167.683	-118.71	1.628	164.024	167.693	-118.72	506749.517	0.438
1.775	0.742	-162.437	-63.796	10.814	-158.436	-62.625	-163.609	506749.517	0.438
1.775	1	9.526	-91.557	11.176	8.279	10.746	-92.778	506749.517	0.438
1.775	1.258	177.272	-122.876	9.182	170.778	177.552	-123.156	506749.517	0.438
0.225	1.408	169.868	-141.101	-0.89	168.996	169.871	-141.104	353528.418	0.422
0.225	1.667	322.67	-101.051	-3.749	321.345	322.703	-101.084	353528.418	0.422

Figure 9 Sample Output; Analysis Results in Tabular Format

Pavement Performance Module

User can view the critical pavement responses; tensile strain at the bottom of the asphalt layer (layer 1) and vertical compressive strain at the top of the subgrade (layer 3 or layer 4 depending on the number of layers initially defined in *General Properties* module).

Critical responses were in turn used to calculate the predicted pavement life in terms of allowable number of standard axle. Two sets of equations proposed by Asphalt Institute and Shell at different reliability levels were used to predict the pavement life. The following Section presents more details on the relationships used to calculate the allowable ESALs.

Mohr-Coulomb yield criterion is used for stability control of the aggregate layers. Mohr-Coulomb parameters namely cohesion and angle of internal friction as well as the depth at which the user selects to perform the stability control are the inputs of this section. More information on the rationale behind the stability control of aggregate layers can be found in the following section.

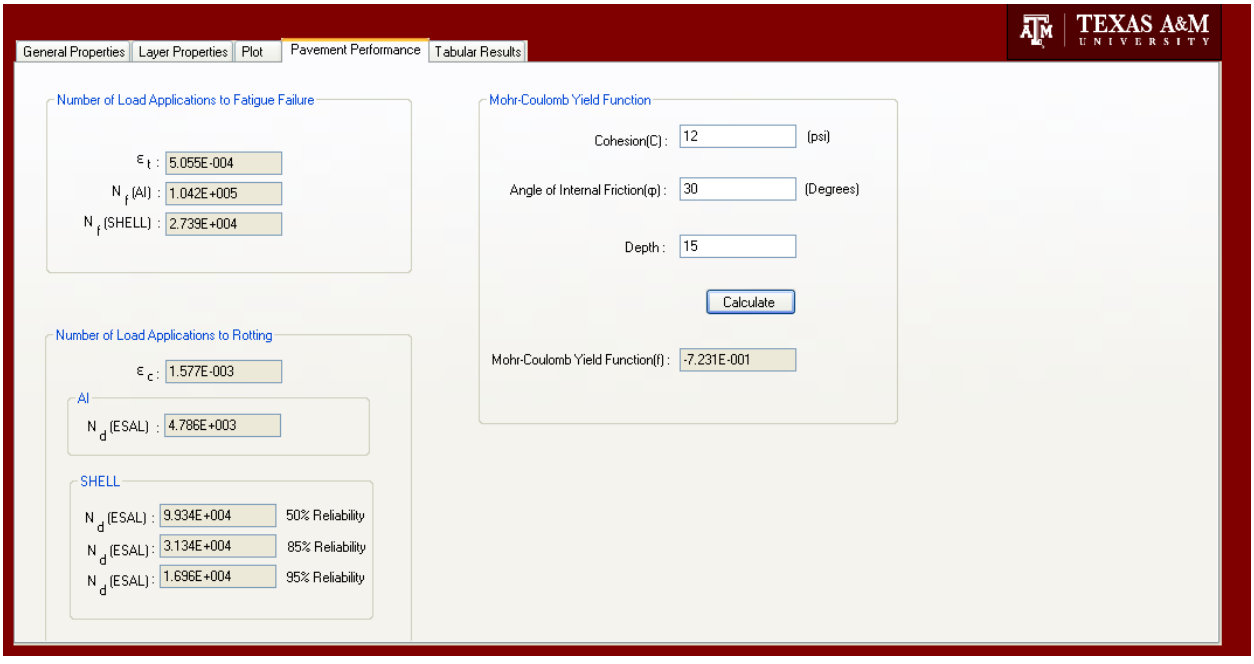

Figure 10 Sample Output; Critical Pavemeent Responses and Predicted pavement Life

Pavement Life Prediction Models

- **Rutting**

This approach relates the number of load applications to failure to stiffness properties and responses of unbound layers subjected to moving wheel loads. The rationale behind these models is to ensure enough cover is present to protect the subgrade layer throughout the expected pavement life. Therefore these models cannot be used to predict the plastic deformations at the top of the subgrade as discussed in previous models.

This type of approach assumes that most of the plastic deformation measured at the pavements surface is due to subgrade deformations, and rutting in structural layers is negligible. The general form of this type of model is presented in equation 2.

$$N_d = \beta\, f_1 (\varepsilon_v)^{f_2} (M_R)^{f_3} \quad (2)$$

N_d= Number of load applications to subgrade failure

f_1, f_2, and f_3=Regression constants

M_R=Resilient modulus of the subgrade soil, psi

ε_v= Plastic strain at the top of the subgrade, in/in

Barker and Brabston used this approach to develop the first generation of limit strain models for the corps of engineers in 1975. In the original formulations, the number of load applications to failure was directly related to the vertical plastic strain at the top of the subgrade (Barker and Brabston 1975). Later Rauhut modified Barkers' equation by considering the effect of subgrade modulus as (Rauhut et al. 1984):

$$N_d = 1.259 \times 10^{-11} (\varepsilon_v)^{-4.082} (M_R)^{0.955} \quad (3)$$

Extensive field studies by several research organizations such as the Asphalt Institute, Belgium Road Research Center, Shell International, and others performed to calibrate this model. The

general form of the model that relates the number of load applications to subgrade distortion to vertical compressive strain at the top of the subgrade is presented in equation 4.

$$N_d = f_4 (\varepsilon_v)^{f_5} \quad (4)$$

Table 1 presents the model parameters based on deflection tolerance and reliability levels in previous studies.

Table 1 Model Parameters and Allowable Rut Depth for Plastic Deformation Models

Organization	**Model Parameter**		**Allowable Rut Depth**
	f_4	**f_5**	**(in)**
Asphalt Institute	1.365×10^{-9}	4.477	0.5
Shell			
50% reliability	6.15×10^{-7}	4.0	0.5
85% reliability	1.94×10^{-7}	4.0	0.5
95% reliability	1.05×10^{-7}	4.0	0.5

- **Fatigue cracking**

Asphalt institute proposed equation 5 to calculate the number load application to reach fatigue failure.

$$N_f = 0.0796 \left(E\right)^{-0.854} \left(\varepsilon_t\right)^{-3.291} \quad (5)$$

Where:

E: Modulus of the asphalt layer (psi)

ε_t: Tensile strain at the bottom of the asphalt layer

Stability Control

This module is developed to ensure the stability of the aggregate layer subjected to heavy loads. TXDOT considers gross vehicle weights ranging from 1112 KN to above 8896 KN as super heavy loads. These loads include industrial equipment and machinery such as dragline components, off-shore pipe laying equipments, oil pressure vessels, and electric transformers. Due to the fact the supper heavy load permit applications have increased significantly during the recent years, it deems necessary to check if the existing pavement is structurally adequate to withstand the supper heavy load. The idea behind this approach is to check if enough cover is present above the subgrade or unbound system so that the stresses are in a tolerable level, and the pavement foundation is protected against rutting (Fernando 1997).

In order to control the stability of the subgrade layer, the pavement response under the super heavy load is calculated. TXDOT procedure employs an incremental, isotropic, nonlinear, layered, and elastic approach to model the unbound aggregate layers. The calculated stresses at the top of the subgrade were in turn used as input to Mohr-Coulomb yield criterion to evaluate the stability of the pavement subjected to a super heavy load. Yield criterion can be expressed as the limit of elastic deformations defined by a combination of stress states (Desai et al. 1987). The Mohr-Coulomb yield function in terms of stress invariants is presented in equation 6.

$$f = \frac{I_1}{3}\sin\varphi + \sqrt{J_2}\sin(\theta + \frac{\pi}{3}) + \frac{\sqrt{J_2}}{3}\cos(\theta + \frac{\pi}{3})\sin\varphi - c\cos\varphi \quad (6)$$

where:

$$\cos 3\theta = \frac{3\sqrt{3}}{2}\frac{J_3}{J_2^{3/2}} = \frac{\sqrt{2}J_2}{\tau_{oct}^3} \quad (7)$$

$$J_2 = \frac{1}{6}\left[(\sigma_1 - \sigma_2)^2 + (\sigma_1 - \sigma_3)^2 + (\sigma_2 - \sigma_3)^2\right] \quad (8)$$

$$J_3 = \left[\sigma_1 - \frac{I_1}{3}\right]\left[\sigma_2 - \frac{I_1}{3}\right]\left[\sigma_3 - \frac{I_1}{3}\right] \quad (9)$$

I_1= First invariant of the stress tensor

J_2 and J_3= Second and third invariants of deviatoric stress tensor

θ= angle of similarity, defined in equation 7

C=cohesion, psi

ϕ= angle of internal friction

σ_1, σ_2 and σ_3= Principal stresses, psi

The potential for damage is assessed based on evaluating the failure function at the top of the subgrade. Several yield criterion are developed by researchers to identify the onset of yielding for different materials. The values of the yield functions can be used as a measure for probability of failure in different materials. Yield functions, specifically developed for granular soils such as Mohr-Coulomb and Lade yield functions clearly show different behavior in compression and tension as indicated by different slopes in compression and tension zones.

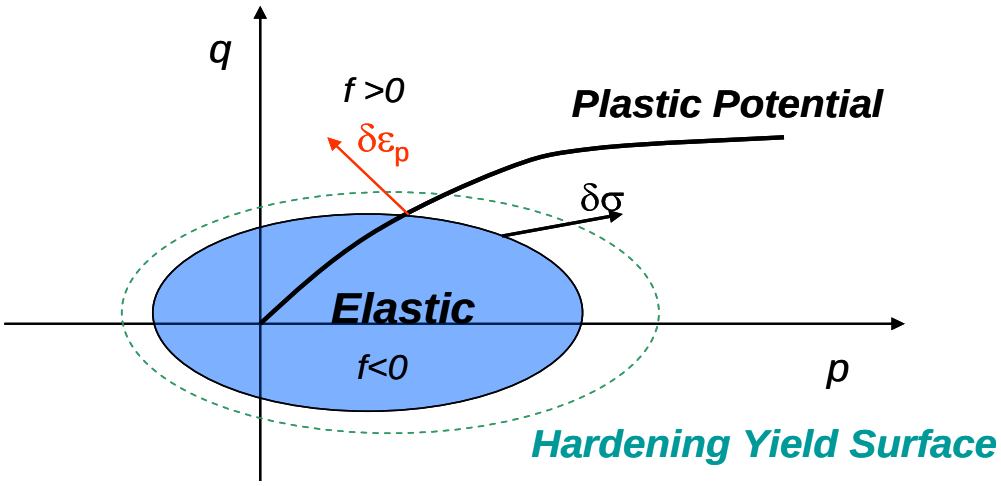

Figure 11 Application of yield function in defining the elastic-plastic boundary

From the mechanics, yielding is signaled when the value of the failure function becomes zero. In other words, if the stress states calculated from the analysis falls inside the yield surface, the value of the yield function is negative and the probability of failure is slim. On the other hand, if the stress states calculated in the analysis part result in positive values of yield function, the pavement system is prone to develop high plastic deformations. This concept is graphically illustrated in figure 11. Figure 12 presents the summary of the protocol for stability control of aggregate layers.

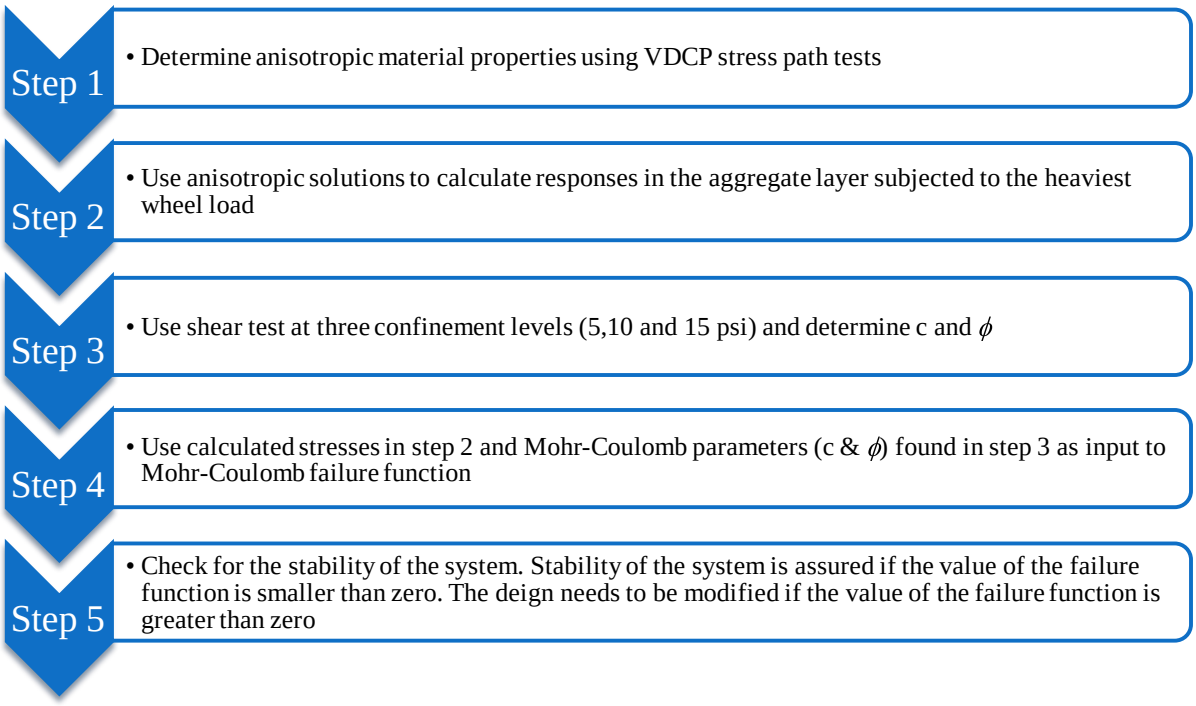

Figure 12 Summary of the Stability Control Protocol for Aggregate Layers